Title

Structural and chemical heterogeneities of primary hyperoxaluria kidney stones from pediatric patients

Journal

Journal of Pediatric Urology, 17(2)

ISSN

1477-5131

Authors

Du, Yuan
Roger, Vincent Blay
Mena, Jorge
et al.

Publication Date

2021-04-01

DOI

10.1016/j.jpurol.2020.11.023

Peer reviewed

Journal of Pediatric Urology (2021) 17, 214.e1–214.e11

Structural and chemical heterogeneities of primary hyperoxaluria kidney stones from pediatric patients

Yuan Du [a,1], Vincent Blay Roger [b,1], Jorge Mena [c], Misun Kang [b], Marshall L. Stoller [c], Sunita P. Ho [b,c,*]

[a]Department of Urology, Beijing Friendship Hospital, Capital Medical University, Beijing, 100050, China

[b]Division of Preclinical Education, Biomaterials & Engineering, School of Dentistry, University of California San Francisco, San Francisco, CA, 94143, USA

[c]Department of Urology, School of Medicine, University of California San Francisco, San Francisco, CA, 94143, USA

* Correspondence to: Sunita P. Ho, 707 Parnassus Avenue, D 3212, UCSF, San Francisco, CA 94143, China.
sunita.ho@ucsf.edu (S.P. Ho)

Keywords
Kidney stones; Hyperoxaluria; XCT; Microscopy; Spectroscopy; Whole-exome sequencing

Received 26 June 2020
Revised 9 November 2020
Accepted 13 November 2020
Available online 20 November 2020

Summary

Objective
Calcium oxalate stones are the most common type among stone-forming patients and in some cases result from predisposed genetic conditions. In this work, we examined the differences in structure and chemical composition between oxalate stones from patients from three groups: 1) pediatric patients that were genetically predisposed (primary hyperoxaluria) to form stones (PPH); 2) control pediatric patients that did not have such genetic predisposition (PN-PH); 3) adult patients that formed oxalate stones without the genetic predisposition (A-CaOx). A variety of instrumental analyses were conducted to identify physicochemical properties of stones characteristic of predisposed pediatric (PPH), pediatric hyperoxaluria (PN-PH), and adult (A-CaOx) patient populations.

Methods
Genetic variants of 16 stone-forming patients were determined using whole-exome gene sequencing. Components of stones from PPH (n = 6), PN-PH (n = 5), and A-CaOx (n = 5) groups were identified using Fourier transform infrared (FTIR) spectroscopy. Stone morphology and density were evaluated using high resolution X-ray computed tomography (micro-XCT). Stone microstructure and elemental composition were mapped with scanning electron microscopy (SEM) and energy dispersive X-ray (EDX) spectroscopy, respectively.

Results
Calcium oxalate bipyramidal crystals were found on stones from all groups. Stones from PPH patients with PH types I and II were composed of calcium oxalate monohydrate (COM) with relatively uniform mineral density (1224 ± 277 mg/cc) and distinct smooth surfaces. By contrast, micro-spherical calcium phosphate particles were found only on PN-PH stones, which also showed a broader range of mineral densities (1266 ± 342 mg/cc). Stones from the PN-PH group also contained phosphorus (P), which was absent in NP-PH stones. A-CaOx stones were of significantly lower mineral density (645 ± 237 mg/cc) than pediatric stones and were more heterogeneous in their elemental composition.

Conclusion
Unique structural and compositional characteristics were identified in stones from pediatric patients with primary hyperoxaluria. These include the absence of phosphorus, a narrower mineral density distribution, and a uniform elemental composition compared to stones from pediatric patients without the genetic predisposition. Thus, characterization of stones at the macro- and micro-scales in combination with genetic testing of patients can provide insights and accurate diagnosis to develop a treatment plan for effective patient care.

[1] both authors contributed equally and are the first authors.

https://doi.org/10.1016/j.jpurol.2020.11.023

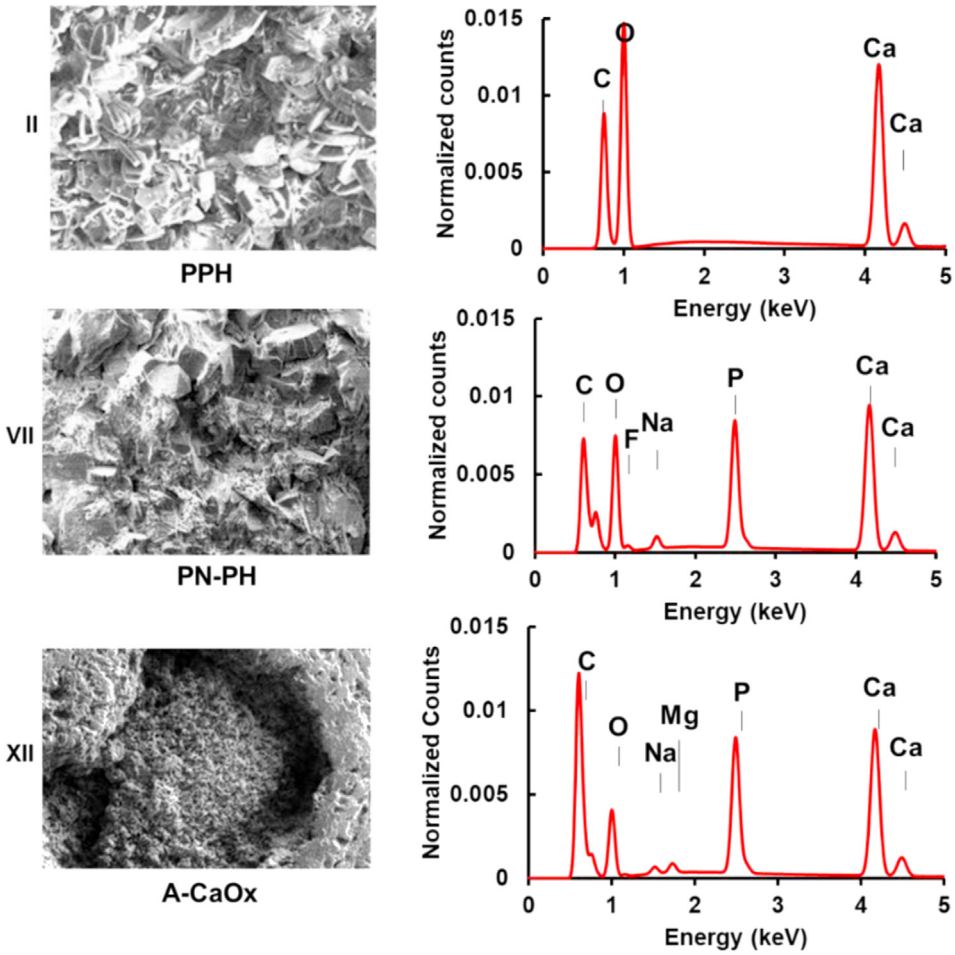

Summary Figure Structure and elemental composition of pediatric primary hyperoxaluria (PPH), pediatric without primary hyperoxaluria (PN-PH), and adult calcium oxalate (A-CaOx) stones.

Introduction

The incidence rates of first-time and recurring kidney stones in pediatric and adult patients have increased globally in the last decade [1—5]. Although the etiology of kidney stone formation in many cases is unknown, a variety of risk factors for kidney stone formation are known, including environment, diet (e.g., secondary hyperoxaluria), microbiota, and various health conditions [6,7]. In some cases, genetic factors can strongly predispose the patient towards stone formation, as in primary hyperoxaluria [6,8]. According to the Genetic and Rare Diseases Information Center, PH is categorized into three types: PH1, PH2, and PH3. PH1 results from a defect in alanine-glyoxylate and serine-pyruvate aminotransferase (AGXT), PH2 results from a defect in glyoxylate and hydroxypyruvate reductase (GRHPR), and PH3 results from a defect in 4-hydroxy-2-oxoglutarate aldolase 1 (HOGA1). PH1 and PH2 are characterized by high concentrations of oxalate in blood and urine [6,8]. Calcium oxalate crystals aggregate in the filtrate that runs through the nephrons and can deposit in the renal tubules. If not managed adequately, over time, this can cause inflammation, impair glomerular filtration [11—13], and have severe health related consequences [9]. Primary hyperoxaluria can result in kidney injury if it is not managed adequately.

PPH may go unrecognized for years as it is not a common occurrence. Monitoring urinary pH, volume, and oxalate and calcium concentrations in addition to genetic testing is the current standard of care to diagnose PH. Genetic testing, however, can be complicated in that not all gene variants are pathological, some variants may still be unknown, and mutations may lie in regulatory sequences of genes beyond the DNA region analyzed [8,9]. Thus, in some cases, liver biopsies are necessary to look for enzyme deficiencies and confirm the diagnosis [10]. Furthermore, external shock-wave lithotripsy should not be used on PPH patients, given the high levels of energy and time needed to fragment oxalate stones, which can damage the kidney in the process [8,14,15]. Thus, it is crucial to identify PH at a younger age. This allows educating the patient by identifying and building personalized protocols to manage the condition and minimize complications such as chronic kidney disease.

Calcium oxalate kidney stones are one of the most common types of kidney stones [4,5]. Most calcium oxalate stones are formed by mono ($C_2H_2CaO_5$) and dihydrate ($C_2H_4CaO_6$) phases, which sometimes are accompanied by calcium phosphates. These calcium oxalate monohydrate (COM) and calcium oxalate dihydrate (COD) phases have a

Table 1 Clinical characteristics of calcium oxalate stone formers in this study.

Specimen	FUR stone composition	Patient age (years)	Gender	8MI (kg/m^2)	Comorbidities	Average mineral density (mg/cc)
1	COM	6	Male	19.0	PH 1	1354
II	COM	8	Male	15.3	PH 1	1097
III	COM	8	Female	18.9	PH 2	1277
IV	COM	5	Male	15.3	PH 2	1460
V	COM	1	Female	15.6	PH 3	1109
VI	COM	2	Male	12.3	PH 3	1218
VII	COD + COM	3	Female	13.5	None	1419
VIII	COD × COM	5	Male	13.0	None	1305
IX	COD + COM	1	Female	16.6	None	1360
X	COM	1	Male	16.4	None	1166
XI	COM + COD	8	Female	18.4	None	1364
XII	COM + COD	66	Male	29.9	None	972
XIII	COM + COD	72	Male	19.0	None	890
XIV	COM + COD	61	Male	36.8	Obesity, hypertension, obstructive sleep apnea	809
XV	COM + COD	39	Male	22.8	Irritable bowel syndrome, hyperlipidemia	663
XVI	COM + COD	65	Male	29.7	Urothelial carcinoma, solitary right kidney	844

microscopically identifiable structure. However, limited information exists on whether primary hyperoxaluria leaves specific physicochemical signatures on stones, particularly in pediatric patients. In this work, we studied calcium oxalate stones removed from pediatric patients with (PPH) and without primary hyperoxaluria (PN-PH), as well as in adult patients (A-CaOx). We hypothesized that differences might exist between stones from these different groups as a result of the genetic predisposition. We combined infrared spectroscopy, high-resolution computerized tomography, electron microscopy, and energy-dispersive X-ray spectroscopy to gain complementary information about the nature of stones in these different groups. Results provided insights into the process of stone formation which could help reduce the number of unrecognized PPH cases that otherwise could go unrecognized and lead to complications later in life.

Materials and methods

Stone specimens

Specimens from pediatric patients included stones and blood. These specimens were collected under protocols approved by the ethics committee of Beijing Friendship Hospital (No. 2015-P2-012-01). All studies involving human participants were performed in accordance with the ethical standards and with the 1964 Helsinki declaration and its later amendments or comparable ethical standards. Inclusion criteria for this study involved primary hyperoxaluria diagnosed by whole-exome sequencing examination and collection of the patients' kidney stones at our centers. Six pediatric calcium oxalate urinary stones from genetically predisposed primary hyperoxaluria patients (PPH), and five calcium oxalate stones from pediatric patients with no known genetic etiology (PN-PH) were obtained from individuals through intra-renal retrograde surgery (IRS) or percutaneous nephrolithotomy (PCNL). Peripheral blood specimens were used for whole-exome gene sequencing. Exclusion criteria for patients' whole-exome sequence examination were no evidence of primary hyperoxaluria or not collected kidney stones. Five adult urinary stone specimens (A-CaOx) were obtained endoscopically from consenting patients undergoing IRS or PCNL following a protocol approved by the University of California San Francisco Committee on Human Research Protection Program (IRB 14—14533). A list of patient characteristics (age, gender, weight, body mass index, comorbidities, and procedure type) and stone specimen characteristics (size, mineral density, and compounds determined by electron microscopy and spectroscopy techniques) are tabulated in Table S1.

Whole-exome gene sequencing

Genomic DNA of the patients and their family members were extracted from peripheral blood using an Omega blood genomic DNA Kit (Omega, D3392). All DNA libraries were prepared following the protocols of Agilent SureSelect QXT Library Prep Kit (5500—0127). Before hybridization, library DNA quantity and quality were assessed with an Agilent Bioanalyzer 2100. Sequencing was performed on an Illumina HiSeq platform using a 2 × 150 bp strategy. All

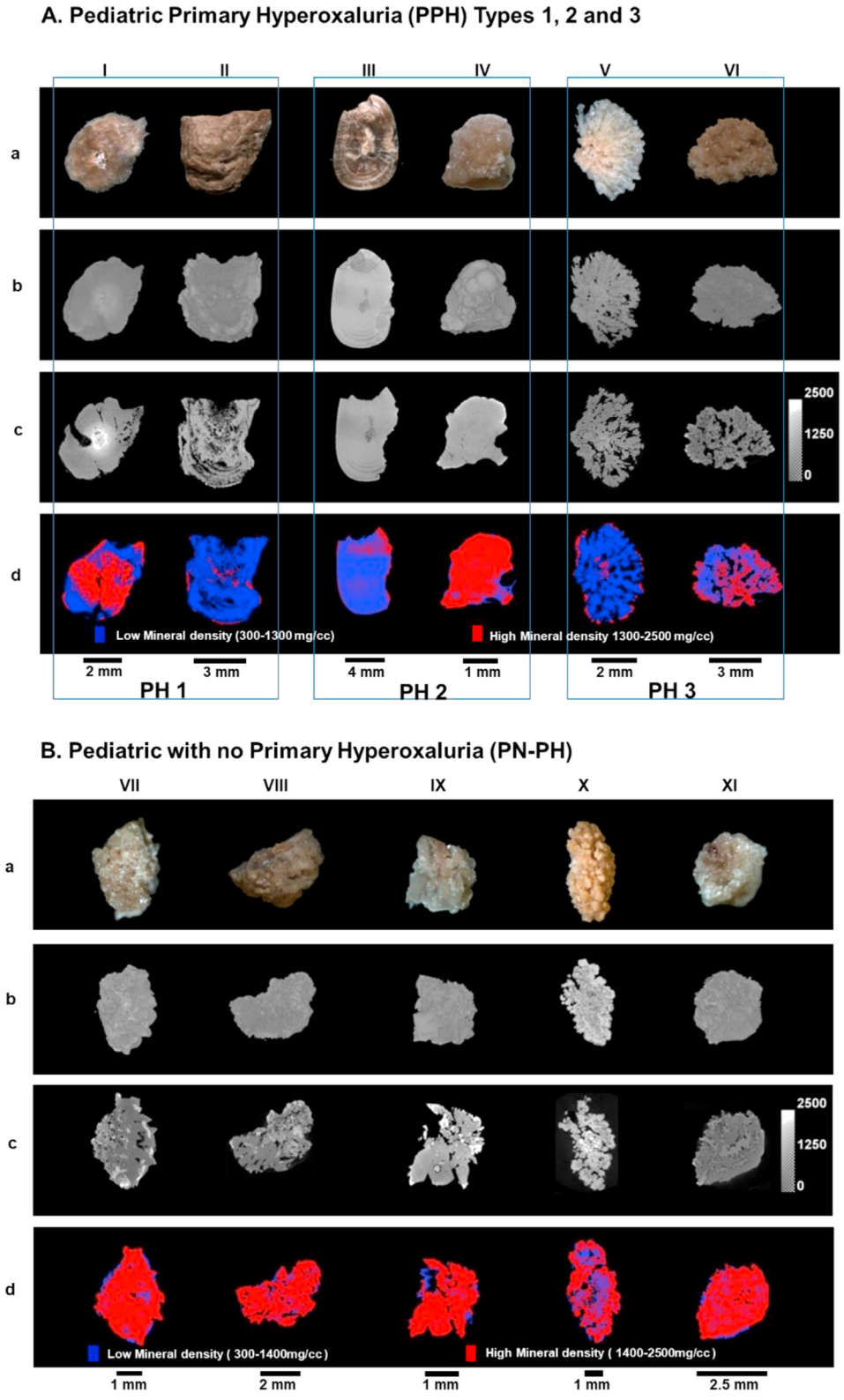

Figure 1 Structure and mineral density distributions in stones from genetically predisposed pediatric primary hyperoxaluria (PPH) patients (A) and pediatric patients without primary hyperoxaluria (PN-PH) (B). In both A and B, the legend for the respective rows are as follows: a) Light microscopy images of representative PPH and PN-PH stone specimens in this study are shown. b) 3D micro-XCT reconstructions of stones and c) selected virtual slices illustrate heterogeneity in mineral densities. d) Slices segmented using density thershold algorithm illustrate higher and lower mineral density regions.

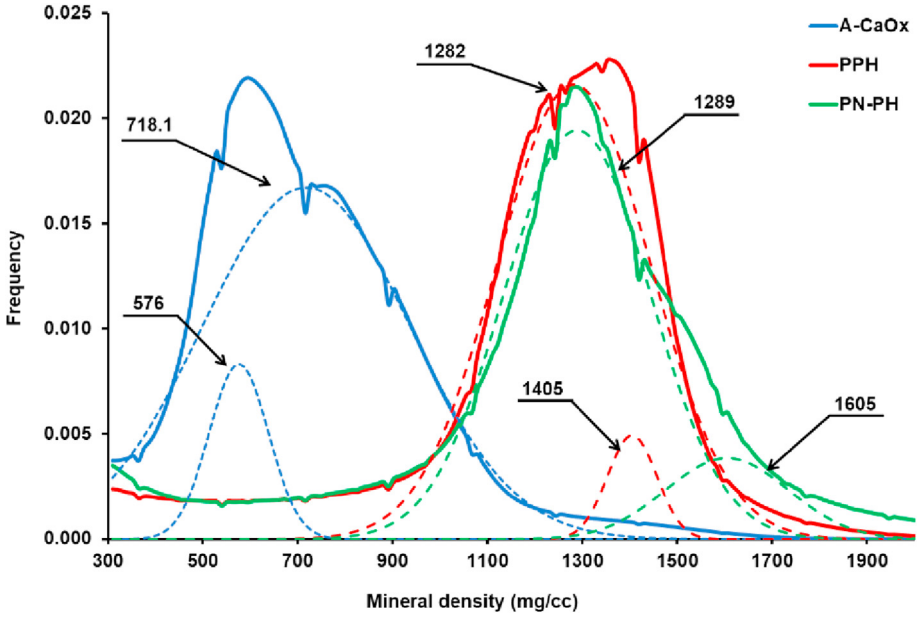

Figure 2 Comparison of the average mineral density distribution across the stone specimens from adult calcium oxalate (A-CaOX), pediatric primary hyperoxaluria (PPH), and pediatric without primary hyperoxaluria (PN-PH) groups. The segmented lines represent Gaussian fits to the average mineral density distributions (mg/cc).

Table 2 Summary characteristics of the mineral density distributions of stones from PPH and NP-PH patients (see Supplemental Fig. 2).

Specimen PPH	**I**	**II**	**III**	**IV**	**V**	**VI**	**Avg. PPH**
Mean (mg/cc)	1341	1063	1269	1413	1076	1175	1224
***s* (mg/cc)**	201	292	133	258	251	297	277
Specimen PN-PH	**VII**	**VIII**	**IX**	**X**	**XI**	**Avg. NP-PH**	
Mean (mg/cc)	1354	1266	1304	1135	1274	1266	
***s* (mg/cc)**	382	345	315	279	339	342	
W statistic	2	***p*-value**	0.0087	**sample estimate difference (mg/cc)**			−86

sequencing reads were quality checked with Trimmomatic [16] using a quality score cutoff of 20 and reads shorter than 40 base pairs were discarded. The remaining reads were aligned to the UCSC human reference genome (hg19, 2005) using the BWA-MEM aligner algorithm [17]. The reads that aligned to the designed target regions were used for subsequent analysis. The consensus sequence and quality of each allele of interest were calculated by GATK [18]. The candidate mutations considered had to pass the following criteria: (i) genotype quality ≥ 20; (ii) sequencing depth ≥ 50; (iii) having a functional consequence, either by affecting gene regulation or its protein product.

Micro X-ray computed tomography of intact stones

Intact stones from patients were scanned at 4× magnification using micro X-ray computed tomography (micro-XCT, Micro-XCT 200, Carl Zeiss Microscopy, Pleasanton, California) with a LE#2 source filter, 40 kVp peak voltage and beam hardening constant of 0.3. Mineral densities of stones in milligrams per cubic centimeter of stone volume (mg/cc) were determined using the watershed algorithm in Avizo software 9.0.2 (FEI, Hillsboro, Oregon) [15]. A Gaussian curve was fitted to the density data using a curve-fitting tool in MATLAB software R2018b (MathWorks Inc., Natick, Massachusetts) to obtain an average mineral density distribution for stones within a group and across groups (PPH, PN-PH, and A-CaOx).

Light microscopy of sectioned stone specimens

Following scanning using micro-XCT, specimens were embedded in LR-white resin (Electron Microscopy Science, Hatfield, Pennsylvania) and were cut into two halves along the long axis of the stone using a slow-speed saw (Isomet, Buehler, Lake Bluff, Illinois). The cut surfaces were ground using a silicon carbide paper with 800 and 1200 grit sizes (Carbimet Paper Strips, Buehler Ltd, Lake Bluff, IL, USA), and finally polished to a mirror-finish with diamond suspension slurry of grades 6, 3, 1, and 0.25 μm (Metadi, Diamond Suspension, H_2O base, Buehler Ltd., Lake Bluff, IL, USA) on polishing cloth (Texmet 1000, Buehler Ltd., Lake Bluff, IL, USA) [19]. All specimens were observed and micrographs of respective structures were recorded using an

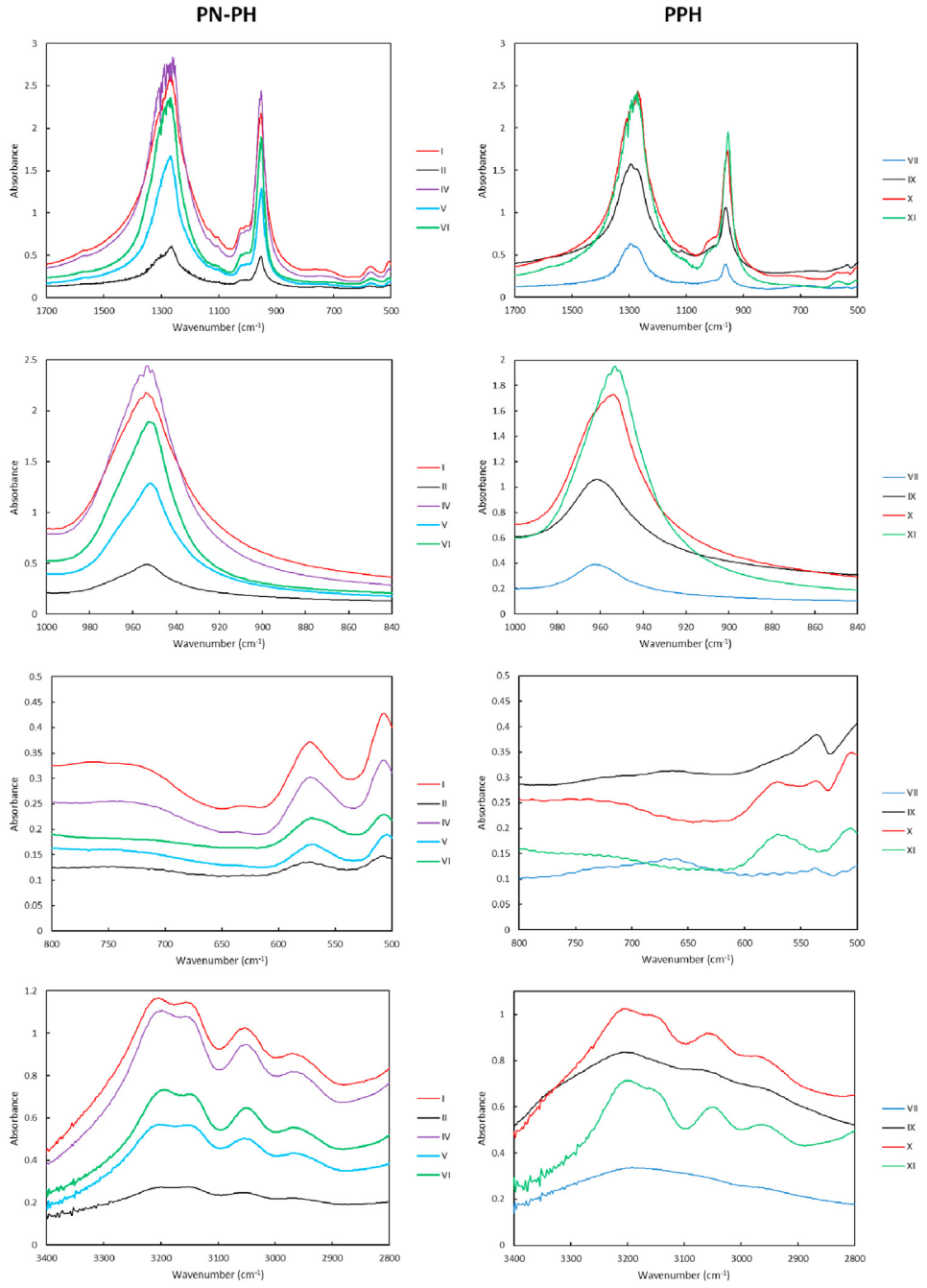

Figure 3 Representative Fourier transform infrared (FTIR) spectra of stones from pediatric primary hyperoxaluria (PPH) and pediatric without primary hyperoxaluria (PN-PH) groups, highlighting different wavenumber regions characteristic of different phases. X-axis: wavenumber (cm^{-1}); Y-axis: absorbance.

optical microscope in reflected mode (BX51, Olympus Scientific Solutions, Waltham, Massachusetts).

Fourier transform infrared spectroscopy of powdered stone specimens

Chemical characterization of stones was performed using powder-Fourier transform infrared (FTIR) (FTIR-7600, Lambda Scientific, China) spectroscopy. The stones were crushed to powder using a mortar and pestle, and were pelleted with potassium bromide (KBr). Spectra were recorded in the range 400—4000 cm^{-1}. Vibrational frequencies characteristic of chemical bonds allowed the identification of various compounds specific to PPH, PN-PH, and A-CaOx stones.

Scanning electron microscopy and energy-dispersive X-ray analysis of sectioned stone specimens

The polished surfaces of the specimens were scanned using a field emission scanning electron microscope (FE-SEM) (Sigma VP500, Carl Zeiss Microscopy, Pleasanton, California) at

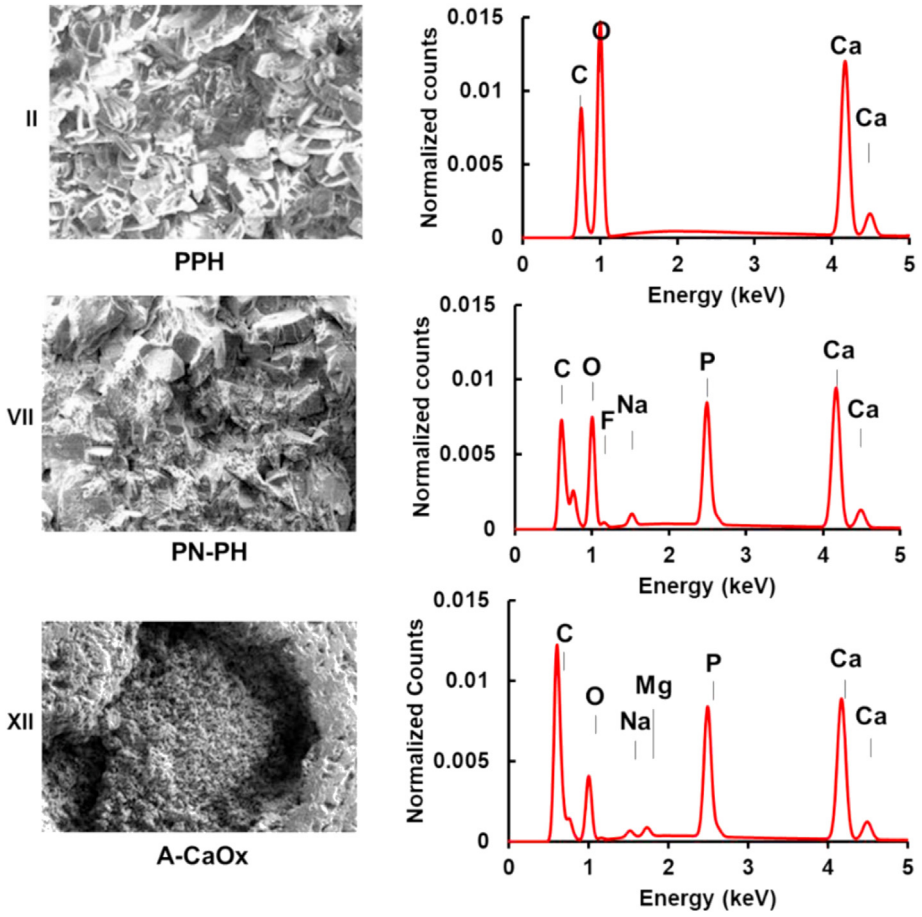

Figure 4 Structure and elemental compositions of pediatric primary hyperoxaluria (PPH), pediatric without primary hyperoxaluria (PN-PH), and adult calcium oxalate (A-CaOx) stones.

1.0 keV. Structures representative of regions (center, middle and edge) within a stone at various magnifications were compared across imaging and spectroscopic data sets. Elemental composition of stones was analyzed using energy-dispersive X-ray spectroscopy (Bruker AXS, Madison, Wisconsin) at a beam energy of 15 keV.

Statistical analysis

Differences between the standard deviations of the mineral density of specimens from both groups were evaluated using an exact one-sided Mann—Whitney—Wilcoxon test, also called Wilcoxon rank-sum test. Notice that in this case, one standard deviation value is derived from each specimen, and thus such standard deviations are considered as independent observations in the analysis. This is a nonparametric test and does not make assumptions about the underlying population distribution of stone densities. Significance of the test was assessed by its p-value.

Results

Primary hyperoxaluria gene mutations

Whole-exome sequencing is a widely used next-generation sequencing (NGS) method that involves sequencing the protein-coding regions of the genome. The human exome represents less than 2% of the genome but contains 85% of currently known disease-related variants, making this method a cost-effective alternative to whole-genome sequencing. Six pediatric patients with primary hyperoxaluria (Table 1) (PPH) were identified and their genotypes, PH1, PH2 or PH3, were confirmed. The mutations are indicated in Table S1 using HGVS nomenclature [20], which describes the specific changes along the gene sequences that are considered relevant with respect to the standard genome (see Methods). One stone specimen from each patient was investigated in detail.

Structural analysis

Light microscopy of stones from all three groups illustrated structural heterogeneity (Fig. 1, Supplemental Fig. 1). Sectioned specimens revealed loose material with small polygonal shaped constituents (I, III, V, Fig. 1). Compared to PH1 and PH2, PH3 specimens presented a branching structure with increased porosity (V, VI). The reconstructed three-dimensional (3D) volumes from micro-XCT virtual slices illustrated smoother peripheries on PH1 and PH2 stones compared to coral-like morphology of PH3 stones (row b in Fig. 1A). Under a light microscope, PN-PH stones illustrated large crystals and abundant voids with no

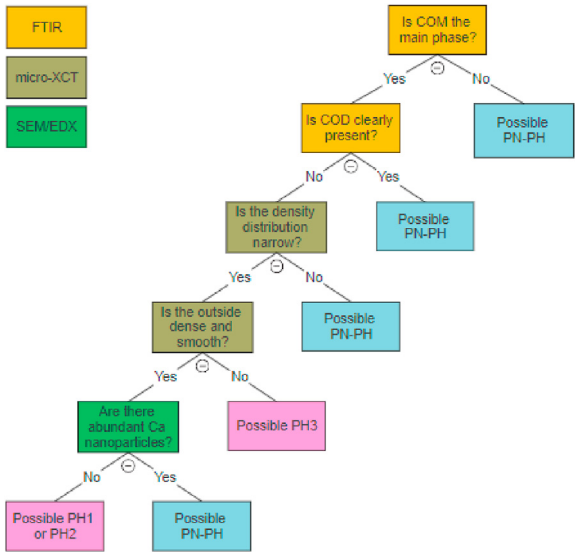

Figure 5 Summary of kidney stone characteristics suggestive of pediatric primary hyperoxaluria (PPH) based on complementary microscopy and spectroscopy techniques used in this study.

significant differences between the volume ratio of mineral to pores in stones between PPH and PN-PH groups.

The structure of stone specimens at a higher resolution was further investigated with the aid of field emission scanning electron microscope (FE-SEM). Main results are shown in Fig. 4 and are supplemented in Supplemental Figs. 3 and 4. Typical calcium oxalate structures were visible in all specimens. Remarkably, spherical nanoparticles of calcium phosphate were observed in all of the PN-PH specimens but were not found in the stones from PPH patients.

Mineral densities

Both PPH and PN-PH stones were segmented into two different mineral density volumes: lower (300—1300 mg/cc, in blue) and higher (1300—2500 mg/cc, in red) mineral densities (row d in Fig. 1A and B). A higher mineral density layer on the outer edges of the stones was observed, and this pattern was predominant in PH3 stones (row d, Fig. 1A). Notably, the spread of the mineral density in stones from the PH group was distinct (Fig. 2); all stones in PPH group presented a narrower mineral density distribution compared to a broader spread for stones in the PN-PH group (see Supplemental Fig. 2). The analysis indicated that stones from the PPH group had a significantly more uniform mineral density than the control ($p < 0.01$), as evaluated by the standard deviation of the mineral density distribution (Table 2). Interestingly, the mineral density of stones from A-CaOx group were significantly lower (576—718 mg/cc) (Fig. 2, Supplemental Fig. S1) compared to stones from both PPH and PN-PH groups (1280—1605 mg/cc) (Table 2, Fig. 2, Supplemental Fig. S2).

Phase composition

Identification of stone composition by IR spectroscopy was performed by automated software, which compares the measured spectrum to a database of spectra of known materials and provides a ranking based on a similarity metric [21], and was then refined by manual analysis of the spectra. In Fig. 3, a few representative spectra illustrate the "fingerprint region" which extends below 1500 cm^{-1} and is particularly useful, as it contains peaks unique to certain compounds. For instance, the absorption bands at 950 and 660 cm^{-1} are specific to COM, whereas bands at 610 and 912 cm^{-1} are specific to COD [22,23]. Ratios of absorption intensities in this region, thus, have been proposed to infer the composition of mixtures [23]. Other features along the spectrum have been reported to be characteristic to COM or COD [24]. The spectrum of a pure calcium oxalate monohydrate shows high absorbances at 1600 cm^{-1} and 1300 cm^{-1}, corresponding to the C═O and C—O stretching vibrations, respectively [25]. In most of our specimens, an absorption peak is present at 1600 cm^{-1}, but it shows a lower intensity than the one at 1300 cm^{-1}. Moreover, we can see that the absorption band characteristic of COD at 912 cm^{-1} is not apparent in either group (Fig. 3), suggesting that all stones contain a considerable fraction of COM. If we look at the region of 800—500 cm^{-1}, we see that the band at 660 cm^{-1} is present in specimens VII and IX, which may suggest that they contain a higher fraction of COM. However, in the 3500-3000 cm^{-1} region, we see multiple peaks characteristic of COM (corresponding to symmetric and antisymmetric —OH stretching [25]) in all the specimens except VII and IX, which display broader spectra more compatible with COD [22]. In fact, this is the criterion often used by clinicians to discern between COM and COD [23]. Additionally, most of the specimens display a weak shoulder at around 1010 cm^{-1}, which could be compatible with the stretching frequency of P—O bonds [25]. Taken together, the data suggest that COM is the main phase across both groups of stones. COD may be present in some of these specimens (particularly VII and IX) and possibly smaller amounts of phosphate. These results are in agreement with the area compositional analyses using EDX, which indicated elemental ratios suggestive of calcium oxalate across all stones. In addition, sodium (Na) and phosphorus (P) were detected in PN-PH stones. Calcium, oxygen, carbon, sodium, and phosphorus were observed in A-CaOx stones (Fig. 4).

Discussion

Kidney stone disease is a globally prevalent condition and occurs in both pediatric and adult populations. COM and/or COD are the most common components of calcium-based stones, which can adhere to epithelia and cell surfaces [26,27]. In this study, six pediatric patients had primary hyperoxaluria as indicated by whole-exome sequencing (Table S1). Of the six PPH patients, two patients per each PH-type were identified (Table S1). The FTIR characterization results in this study agree with previous reports in that kidney stones of PH patients typically consist of >95% COM [8]. Indeed, all PH specimens in this work seemed to consist mainly of COM based on their IR absorption spectra (Fig. 3), and only with electron microscopy at a higher resolution could regions of calcium phosphate be detected, particularly among PN-PH patients. The crystal facets

observed in our results (Fig. 4, Supplemental Figs. 3 and 4) exhibit sharp edges that might physically damage renal epithelial cells [27,28]. Calcium oxalate crystals are also known to induce the generation of reactive oxygen species (ROS) by cells and trigger biochemical cascades resulting in apoptosis [29].

Investigating the uroliths using micro-XCT led to very interesting results. Some characteristics of the density distributions are summarized in Table 2. A notable difference is that stones from PPH patients have a significantly narrower density distribution than those from PN-PH ($p < 0.01$) (Table 2, Fig. 2, Supplemental Fig. S2). A narrower distribution may be related to a higher supersaturation of calcium oxalate induced by the condition, in the form of higher and possibly more constant levels of urinary oxalate than in patients without primary hyperoxaluria [10,30,31]. Indeed, in the case of PH1 and PH2, which cause increased oxalate excretion compared to PH3, the external surfaces were smoother compared to stones from PH3 patients. This smoothness is unusual and had been previously associated with primary hyperoxaluria [32,33]. These observations also agree with previous reports on crystal morphologies in kidney stones [21,34].

The whewellite (COM) stones from PH3 patients, at least in this study, displayed unique characteristics in that they were more porous and illustrated higher mineral density on their periphery. These differences may be related to different levels of urinary oxalate in these patients compared to PH1 and PH2. Their branching structure may help explain why PH3 specimens break and are passed out by urine. PH3 mutations manifest early in life, with high stone recurring rates, although the renal function tends to be much better preserved compared to PH1 and PH2 [35–37]. Higher amounts of calcium oxalate are generated through liver metabolism, leading to crystal aggregation and adhesion in the kidney. In fact, in advanced cases of end-stage renal disease, PH1 and PH2 patients could be in the need of kidney and/or liver transplants due to systemic oxalate crystallization, while there have been no such cases reported for PH3 patients [8]. On the other hand, small phosphate particles were barely detectable in stones from the PH group, which further suggests that the stones formed more rapidly from higher concentrations of calcium oxalate. In a study by Daudon and coworkers [38], a radiating coral-like structure was also observed in PH2 stones. Coral-like structures seem to be associated with higher concentrations of calcium oxalate crystals. By contrast, stones from the PN-PH group displayed many calcium phosphate particles of different morphologies, which are also found in hypercalciuria and idiopathic calcium-based stones [15,19].

Taken together, the results of this study indicate that kidney stones from pediatric primary hyperoxaluria patients (PPH) have detectable and distinctive physicochemical features compared to control pediatric patients (PN-PH). As summarized in Fig. 5, microscopy and spectroscopy techniques can help identify primary hyperoxaluria, had it not been identified previously, and provide mechanistic insights into degree of hyperoxaluria condition and stone formation. FTIR can be used to assess the most abundant mineral phases present in the stone. In this study, we have found that COM is the main phase formed by pediatric patients with primary hyperoxaluria, whereas, in other individuals, small amounts of COD are usually detected accompanying COM. By using micro-XCT, the density distribution of the calculi can be evaluated. Our results indicate that pediatric PH stones display a more uniform mineral density, whereas stones from other patients generally span a significantly broader mineral density range. Morphological observations can also strengthen some of these conclusions, as described in other studies [34,38]. Lastly, EM and EDX allow observation of microstructural features and chemical composition that seem characteristic of pediatric PH patients, including lower levels of phosphorus or other elements.

The results of this study also suggest that stones from adults exhibit significantly lower mineral density than stones from pediatric patients (Fig. 2, Supplemental Fig. 1). A-CaOx stones displayed a more diverse elemental composition (Fig. 4, Supplemental Figs. 3 and 4), similar to PN-PH stones. Although the adult group in this study came from a different geographic region, we hypothesize that the increased serum calcium concentration in children that supports the development of bone may contribute to the observed higher mineral densities of stones in pediatric patients [39,40], although further studies are needed to validate this.

Some limitations of our study include: 1) a limited number of stones for each group given the rarity of the condition. We thus hope that these first results will stimulate other researchers to validate and extend them. 2) Some of the pediatric specimens were stone fragments instead of intact stones, which may limit the ability to identify other plausible structural features. 3) Complete urine metabolic evaluations were not measured routinely, consequently reducing our understanding of the role of urinary uric acid, citrate, phosphate, and potassium in stone development. Other limitations include 4) the lack of preoperative clinical data, and 5) the geographic heterogeneity of the non-PPH population.

Based on this study, we encourage gene sequencing to be conducted before surgery on pediatric patients presenting bilateral kidney stone, at least for the genes AGXT, HOGA1 and GRHPR. Ideally, whole-exome sequencing is proposed as the standard of care in the near future. This test is current practice at our institutions: it requires 4 ml of blood, and costs less than $500 (Bestnovo and Candygene prices). We also encourage, when the surgical intervention allows, stone fragment collection to enable additional analyses. The findings of this work could be used, and are not to replace, but to complement sequencing tests. Sequencing results exclusively are not conclusive of patients' conditions. All tests have false positives and false negatives, and expanding the observations in this study to a larger pool of patients may help validate these findings with an overall objective to improve current diagnostics.

Conclusions

Primary hyperoxaluria is a relatively unusual condition, even among the pediatric population. However, if it is not recognized and managed earlier on, it can lead to chronic kidney disease and devastating health problems. In this

work, we characterized a set of stones from pediatric PH and non-PH patients using complementary tomography, microscopy, and spectroscopy techniques, which are becoming increasingly available in laboratories affiliated with hospitals and clinics. This complete characterization reveals that certain stone features (uniform mineral density, microscopically and spectroscopically absent calcium phosphate particulates, smooth surface, absence of phosphorus) collectively can be used as an indicator for genetically predisposed primary hyperoxaluria condition. This set of distinctive characteristics or "signature" is likely a consequence of the unique oxalate profile in urine in children with primary hyperoxaluria and it can provide hints to the clinician about the presence of the condition. Lastly, we have also identified notable differences between stones from adult and pediatric patients in terms of density and composition, which may be influenced by developmental, dietary, and environmental factors. It is important to understand these differences across stone types so that stone formation can be best managed and prevented. We recommend whole-exome gene sequencing to be conducted on both pediatric and adult patients suffering from oxalate kidney stones to enable optimal management and preserve renal health.

Conflicts of interest

There are no conflicts of interest to declare.

Acknowledgements

The authors would like to thank Grace Nonomura for help with specimen preparation. The authors thank the Biomaterials and Bioengineering Correlative Microscopy Core (http://bbcmc.ucsf.edu), UCSF for the use of their MicroXCT-200 and SIGMA 500-VP Field Emission Electron Microscope — Scanning and Transmission. This work was supported by the National Institute of Health [R21 DK109912 (SPH,MLS); R01 DE022032 (SPH)].

References

[1] Scales CD, Smith AC, Hanley JM, Saigal CS. Prevalence of kidney stones in the United States. Eur Urol 2012;62(1):160—5.
[2] Edvardsson VO, Ingvarsdottir SE, Palsson R, Indridason O. Incidence of kidney stone disease in Icelandic children and adolescents from 1985 to 2013: results of a nationwide study. Pediatr Nephrol 2018;33(8):1375—84.
[3] Tiselius HG. Epidemiology and medical management of stone disease. BJU Int 2003;91(8):758—67.
[4] Khan SR, Pearle MS, Robertson WG, Gambaro G, Canales BK, Doizi S, et al. Kidney stones. Nat. Rev. Dis. Primers 2016;2:16008.
[5] Blay V, Li MC, Ho SP, Stoller ML, Hsieh HP, Houston DR. Design of drug-like hepsin inhibitors against prostate cancer and kidney stones. Acta Pharm Sin B 2020;10(7):1309—20.
[6] Williams HE, Smith Jr LH. Disorders of oxalate metabolism. Am J Med 1968;45(5):715—35.
[7] Tavasoli S, Alebouyeh M, Naji M, Shakiba Majd G, Shabani Nashtaei M, Broumandnia N, et al. Association of intestinal oxalate-degrading bacteria with recurrent calcium kidney stone formation and hyperoxaluria: a case—control study. BJU Int 2020;125(1):133—43.
[8] Cochat P, Rumsby G. Primary hyperoxaluria. N Engl J Med 2013;369:649—58.
[9] Hulton SA. The primary hyperoxaluria: a practical approach to diagnosis and treatment. Int J Surg 2016;36:649—54.
[10] Bhasin B, Ürekli HM, Atta MG. Primary and secondary hyperoxaluria: understanding the enigma. World J Nephrol 2015;4(2):235—44.
[11] Verhulst A, Asselman M, Persy VP, Schepers MS, Helbert MF, Verkoelen CF, et al. Crystal retention capacity of cells in the human nephron: involvement of CD44 and its ligands hyaluronic acid and osteopontin in the transition of a crystal binding into a nonadherent epithelium. J Am Soc Nephrol 2003;14:107—15.
[12] Schepers MS, van Ballegooijen ES, Bangma CH, Verkoelen CF. Crystals cause acute necrotic cell death in renal proximal tubule cells, but not in collecting tubule cells. Kidney Int 2005;68:1543—53.
[13] Salido E, Pey AL, Rodriguez R, Lorenzo V. Primary hyperoxaluria: disorders of glyoxylate detoxification. Biochim Biophys Acta 2012;1822:1453—64.
[14] Carrasco Jr A, Granberg CF, Gettman MT, Milliner DS, Krambecka AE. Surgical management of stone disease in patient with primary hyperoxaluria. Urology 2015;85(3):522—6.
[15] Sherer BA, Chen L, Yang F, Ramaswamy K, Killilea DW, Hsi RS, et al. Heterogeneity in calcium nephrolithiasis: a materials perspective. J Mater Res 2017;32(1314):2497—509.
[16] Bolger AM, Lohse M, Usadel B. Trimmomatic: a flexible trimmer for Illumina sequence data. Bioinformatics 2014;30(15):2114—20.
[17] Li H, Durbin R. Fast and accurate long-read alignment with Burrows Wheeler transform. Bioinformatics 2010;26(5):589—95.
[18] McKenna A, Hanna M, Banks E, Sivachenko A, Cibulskis K, Kernytsky A, et al. The Genome Analysis Toolkit: a Map Reduce framework for analyzing next-generation DNA sequencing data. Genome Res 2010;20(9):1297—303.
[19] Sherer BA, Chen L, Kang M, Shimotake AR, Wiener SV, Chi T, et al. A continuum of mineralization from human renal pyramid to stones on stems. Acta Biomater 2018;71:72—85.
[20] den Dunnen JT. Sequence variant descriptions: HGVS nomenclature and mutalyzer. Curr. Protoc. Hum. Genet. 2016;90:7.13.1—7.13.19.
[21] Gervasoni J, Primiano A, Ferraro PM, Urbani A, Gambaro G, Persichilli S. Improvement of urinary stones analysis combining morphological analysis and infrared spectroscopy. J chem (Hindawi) 2018;2018:4621256.
[22] Mandel G, Mandel N. Analysis of stones. In: Coe FL, Favus MJ, Pak CYC, Park CH, editors. Kidney stones: medical and surgical management. Philadelphia: Lippencott-Raven; 1996. p. 323—35.
[23] Lin MH, Song YL, Lo PA, Hsu CY, Lin ATL, Huang EYH, et al. Quantitative analysis of calcium oxalate hydrate urinary stones using FTIR and 950/912 cm—1 peak ratio. Vib Spectrosc 2019;102:85—90.
[24] Sekkoum K, Cheriti A, Taleb S, Belboukhari N. FTIR spectroscopic study of human urinary stones from El Bayadh district (Algeria). Arab. J. Chem. 2016;9:330—4.
[25] Asyana V, Haryanto F, Fitri LA, Ridwan T, Anwary F, Soekersi H. Analysis of urinary stone based on a spectrum absorption FTIR-ATR. J Phys: Conf. Ser. 2016;694:012051.
[26] Manissorn J, Fong-Ngern K, Peerapen P, Thongboonkerd V. Systematic evaluation for effects of urine pH on calcium oxalate crystallization, crystal-cell adhesion and internalization into renal tubular cells. Sci Rep 2017;7(1):1798.

[27] Sun XY, Xu M, Ouyang JM. Effect of crystal shape and aggregation of calcium oxalate monohydrate on cellular toxicity in renal epithelial cells. ACS Omega 2017;2(9):6039—52.
[28] Chu Z, Zhang S, Zhang B, Zhang C, Fang CY, Rehor I, et al. Unambiguous observation of shape effects on cellular fate of nanoparticles. Sci Rep 2014;4:4495.
[29] Sun XY, Ouyang JM, Yu K. Shape-dependent cellular toxicity on renal epithelial cells and stone risk of calcium oxalate dihydrate crystals. Sci Rep 2017;7(1):7250.
[30] Robijn S, Hoppe B, Vervaet BA, D'Haese PC, Verhulst A. Hyperoxaluria: a gut—kidney axis? Kidney Int 2011;80(11):1146—58.
[31] Lumlertgul N, Siribamrungwong M, Jaber BL, Susantitaphong P. Secondary oxalate nephropathy: a systematic review. Kidney Int. Rep. 2018;3(6):1363—72.
[32] Williams JC, Worcester E, Lingeman JE. What can the microstructure of stones tell us? Urolithiasis 2017;45(1):19—25.
[33] Daudon M. Analyse et classification des calculs: contribution à l'etiologie de la maladie lithiasique. Rev Med Suisse 2004;124(8):445—53.
[34] Cloutier J, Villa L, Traxer O, Daudon M. Kidney stone analysis: "Give me your stone, I will tell you who you are!". World J Urol 2015;33(2):157—69.
[35] Sayer JA. Progress in understanding the genetics of calcium-containing nephrolithiasis. J Am Soc Nephrol 2017;28(3):748—59.
[36] Hopp K, Cogal AG, Bergstralh EJ, Seide BM, Olson JB, Meek AM, et al. Rare Kidney Stone Consortium. Phenotype-genotype correlations and estimated carrier frequencies of primary hyperoxaluria. J Am Soc Nephrol 2015;26(10):2559—70.
[37] Hoppe B. An update on primary hyperoxaluria. Nat Rev Nephrol 2012;8(8):467.
[38] Daudon M, Jungers P, Bazin D. Peculiar morphology of stones in primary hyperoxaluria. N Engl J Med 2008;359(1):100—2.
[39] Lietman SA, Germain-Lee EL, Levine MA. Hypercalcemia in children and adolescents. Curr Opin Pediatr 2010;22(4):508—15.
[40] Penido MGMG, de Sousa Tavares M. Pediatric primary urolithiasis: symptoms, medical management and prevention strategies. World J Nephrol 2015;4(4):444—54.

Appendix A. Supplementary data

Supplementary data to this article can be found online at https://doi.org/10.1016/j.jpurol.2020.11.023.

Nomenclature

A-CaOx	Adult Calcium Oxalate
AGXT	Alanine-glyoxylate and serine-pyruvate aminotransferase
BMI	Body mass index
CaOx	Calcium oxalate
CaP	Calcium phosphate
COD	Calcium oxalate dihydrate
COM	Calcium oxalate monohydrate
EDX	Energy-Dispersive X-ray
GARD	Genetic and Rare Diseases Information Center
GFR	Glomerular filtration rate
GRHPR	Glyoxylate and hydroxy-pyruvate reductase
HOGA1	4-hydroxy-2-oxoglutarate aldolase 1
Micro-XCT	High-resolution X-ray computed tomography
PH	Primary hyperoxaluria
PH1	Primary hyperoxaluria type I
PH2	Primary hyperoxaluria type II
PH3	Primary hyperoxaluria type III
PN-PH	Pediatric without primary hyperoxaluria
PPH	Pediatric primary hyperoxaluria
ROS	Reactive oxygen species
SEM	Scanning Electron Microscopy